

BACHELOR'S PROJECT
UNIVERSITY OF COPENHAGEN

COUPLING OF AN LC-CIRCUIT TO A NANOMECHANICAL MEMBRANE

AUTHOR:
Yeghishe Tsaturyan

SUPERVISOR:
Anders Sørensen

JUNE 15, 2012

Contents

1	Introduction	3
1.1	Cavity optomechanics	3
1.2	The setup of this study	5
2	Fundamentals	7
2.1	Brownian motion and classical Langevin equation	8
2.2	Quantum theory of beam splitters	8
2.3	Quantum Langevin equation	9
2.4	Fourier analysis	12
3	Analysis I: weak-coupling regime	13
3.1	The rotating-wave approximation	14
3.2	Simple limiting cases	14
3.3	Full derivation	17
4	Analysis II: strong-coupling regime	22
4.1	Looking at the general picture	23
4.2	Break-down of the rotating-wave approximation	24
5	Discussion and outlook	28
6	Conclusion	28
A	Solutions with RWA	30
B	Entries of the inverted 4x4 matrix	31
C	Solutions without RWA	32

Summary

In recent years significant progress has been made in the emerging research field of optomechanics, promising to unlock the door towards exploration of micro- and nanomechanical objects in the quantum-regime. Advances in optomechanical coupling and, most importantly, cooling of high-quality mechanical systems have not gone unnoticed, and many exciting ideas on exploiting optomechanical cooling have been proposed. Among these is a proposal by A.S. Sørensen, E.S. Polzik and collaborators, suggesting to extend the "standard" optomechanical setup to electrical circuits. By coupling a high-quality nanomechanical membrane to an LC-circuit, the electrical circuit can be effectively cooled. This is the main idea presented in the paper by the above mentioned[1], and is the starting point of this project.

In this bachelor's thesis the main results of the paper are presented, and a full derivation is carried out, both with and without the rotating-wave approximation (RWA). The occupation number of the LC-circuit is calculated using the Heisenberg-Langevin approach to quantum damping, and the results are compared to those in the paper.

Furthermore, we review the basics of optomechanical cooling, and the quantum mechanical description of damping is introduced.

Resumé

I løbet af de seneste år har der været store fremskridt inden for området *optomekanik* og der er håb for at kunne være i stand til at undersøge, hvordan mikro- og nanomekaniske objekter opfører sig kvantemekanisk. Fremskridt inden for optomekanisk køling er alt andet end blevet overset og der er blevet foreslået en række spændende eksperimenter, der udnytter optomekanisk køling. Blandt disse er et forslag af bl.a. A.S. Sørensen og E.S. Polzik[1], hvor en udvidelse af den velkendte optomekaniske opstilling bliver beskrevet. Ved at koble en nanomekanisk membrane af høj Q-værdi til et LC-kredsløb kan man opnå en effektiv køling af kredsløbet. Denne ide ligger til grund for denne afhandling.

I dette bachelorprojekt vil hovedresultaterne fra artiklen skrevet af A.S. Sørensen og E.S. Polzik blive præsenteret, samt den fulde udledning for koblingen mellem den nanomekaniske membran og LC-kredsløbet vil blive præsenteret. Disse resultater vil blive sammenlignet med de approksimative fra artiklen.

Derudover vil der blive givet et generelt overblik over konceptet optomekanisk køling og den kvantemekaniske beskrivelse af dæmpning vil blive præsenteret.

1 Introduction

Since the early days of quantum mechanics, scientists have been intrigued by the differences between the classical and quantum world. Upon entering the world of quantum mechanics, objects exhibit quite bizarre behavior, different from the everyday world. But despite the fact that scientists have carried out countless experiments exhibiting quantum behaviour of light and matter, one question remains unanswered: where does the classical world "end" and the quantum world "begin"? And can macroscopic objects behave quantum mechanically? These and many other questions can potentially be answered within a relatively new field called *optomechanics*.

Optomechanics is at the intersection of quantum optics and nanophysics, dealing with the interaction of light and a mechanical oscillator (e.g. a mirror attached to a spring or a cantilever). Due to a specific type of interaction, namely the radiation pressure force, the center-of-mass motion of such an oscillator can be *cooled*.

The fact that electromagnetic radiation can exert forces on material objects can be traced back to Maxwell, yet, there would have to go over a century before the pioneering work of V.B. Braginsky and A. Manukin in the late 1960's [2]. Their study of radiation pressure effects on a mirror attached to a mechanical oscillator put the foundation for optomechanics as it is known today. The following is a brief overview of the basics of cavity optomechanics.

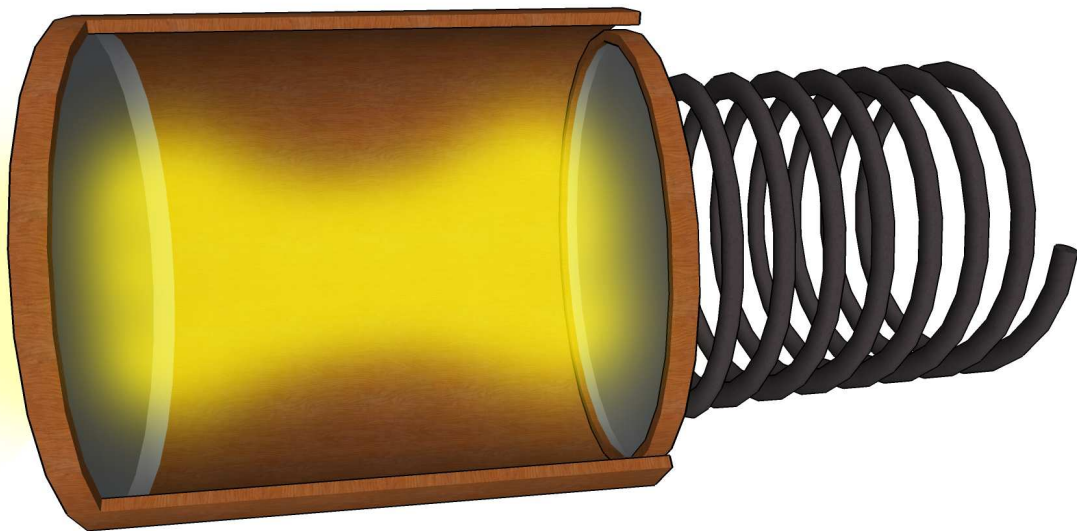


Figure 1: Cavity with a movable end-mirror.

1.1 Cavity optomechanics

It is a well-known fact that a light beam of power P incident on a perfect reflector (e.g. a high-quality mirror) will exert a force $F = 2P/c$ on the object. Now, let us imagine that our mirror is suspended on a spring and places as one of the end mirrors of a cavity (i.e. a Fabry-Perot resonator), such that one of the mirrors is static and the other

movable (see Figure 1). The light will be retroreflected multiple times¹ before escaping the cavity. Thus the light intensity inside of our cavity will be resonantly enhanced, resulting in a greater radiation pressure force on the movable mirror. Ultimately we wish to use the resonant enhancement to cool the motion of our oscillator, much like cooling of atoms using radiation pressure. But in contrast to the optical trapping of individual atoms, current research on cavity optomechanics is dealing with cooling of micro- or nanomechanical oscillators consisting of approximately 10^{14} atoms!

We start by considering our cavity. For now let us think of the movable mirror as static. Depending on the length of the resonator, light of certain frequencies will interfere constructively or destructively. To be more specific, when the cavity length equals an integer multiple of half of the wavelength, $L = n\lambda/2$, we have a standing wave inside of the cavity. Using the relation between wavelength and frequency², $\lambda = c/\nu$, we can easily find the "allowed" frequencies

$$\nu = \frac{c}{2L}n \quad (1)$$

One should note that the mode spacing, also known as the *free spectral range* (FSR), is $\Delta\nu = c/2L$.

But due to the fact that one of the mirrors in our cavity is not a perfect reflector, frequencies in the vicinity of the "allowed" frequencies are present inside our cavity (see Figure 2). The full-width at half-maximum (FWHM) of each peak is related to the reflectivity of the semi-transparent mirror and hence the life-time of photons inside the cavity [3, p.225]. The higher reflectivity, the narrower peak.

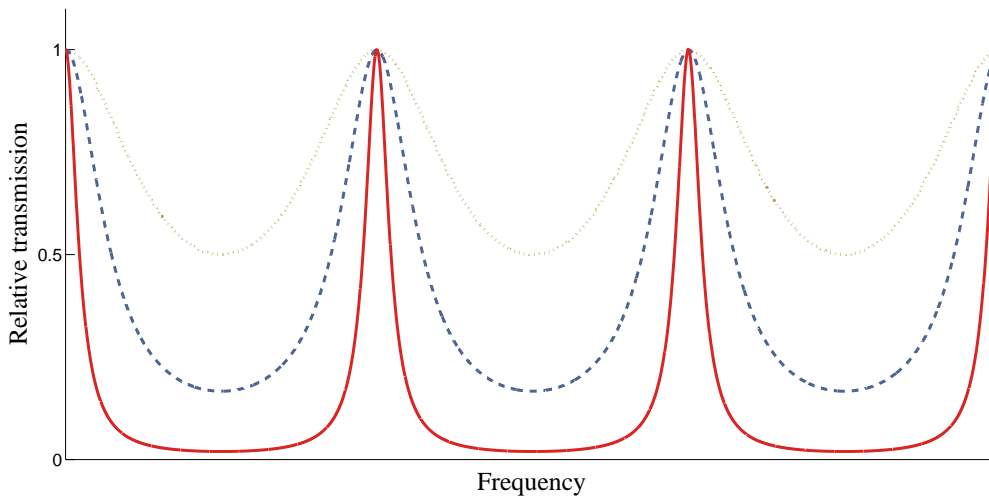


Figure 2: Relative intensity transmission for a Fabry-Perot resonator as a function of frequency. The transmission spectra for three different reflectivities are illustrated. If an incoming monochromatic light is on resonance (in accordance to eq. (1)), the transmitted (i.e. output) light field will have the same intensity as the input.

¹Assuming that the life-time of photons inside the cavity is comparable to or longer than the roundtrip time.

²Under the assumption that we have vacuum inside the cavity.

The last detail in our simplified picture of optomechanical cooling is the laser, which will be driving our cavity. We are now ready to consider the effect of an oscillating mirror. Let us imagine that the laser is red-detuned³ with respect to the cavity and note that an elongation of the cavity results in a decrease in the optical resonance frequency. The movable mirror is originally in its equilibrium position, but as the laser is turned on, the end-mirror starts to move. As it moves to the right (hence elongating the cavity), the optical resonance frequency decreases, approaching the laser frequency. Similarly, the intensity in the cavity increases and following eq. (1), so does the radiation pressure force. But due to the finite decay time of the intercavity field, the radiation pressure force is *retarded*⁴, meaning that the force upon the end-mirror will be at its maximum as the mirror moves *back* towards the equilibrium position, hence extracting mechanical energy from the oscillator and thereby cooling the motion of the oscillator. The intensity in the cavity depends very sensitively on the position of the movable mirror. Thus a change in the position affects the intercavity intensity, which in return affects the motion of the oscillator - an effect also known as "dynamical back-action". We say that the oscillator is *coupled* to the cavity (field).

Following the same line of thought, one could convince himself/herself that if the laser was blue-detuned in relation to the optical resonance, we would have amplification instead of cooling.

Despite its simplicity, the explanation above provides the basic idea to the optomechanical cooling effect. We have seen that for a certain laser detuning one can actually cool the motion of a mechanical oscillator⁵. And although it is not the objective of this thesis carry out a detailed analysis of radiation pressure cooling of a mechanical oscillator, it is important to know the basics about this.

1.2 The setup of this study

The experimental setup illustrated in Figure 1 has up to now our toy example. But now, as we have understood the basic idea of cooling, we are ready to move on to the setup, which will be the focus of our study throughout this thesis. To begin with, we replace the moving mirror with static mirror and place a semi-transparent dielectric nanomechanical membrane inside our cavity. Although this configuration may seem significantly different from the one previously examined, the physics is essentially the same. Finally, we introduce two capacitor plates in this picture, one on each side of the membrane - these will be part of an LC-circuit. One of the capacitor plates is in fact a set of wires, which can be thought of as a "fork capacitor" (see figure below). In this configuration the capacitance will be dependent on the membrane position⁶. The LC-circuit is thus *coupled* to the mechanical oscillator.

Due to this coupling, the LC-circuit is being cooled alongside with the mechanical os-

³The laser is tuned to a frequency below the resonant frequency of the cavity.

⁴The photons are still in the cavity for a period of time, after the mirror has moved.

⁵Notice that optomechanical cooling does not reduce the bulk temperature, rather the effective temperature of the oscillator.

⁶Based on simple symmetry considerations one could convince himself/herself that in the case of two normal capacitor plates the capacitance would be independent on the position

cillator. The reason why this setup is particularly interesting is due to the fact that LC-circuits are used in a wide variety of settings, and cooling of such systems would without any doubt be widely applicable. This thesis aims to provide a quantum mechanical description of this coupling. We wish to find out how the LC-circuit can be effectively cooled.

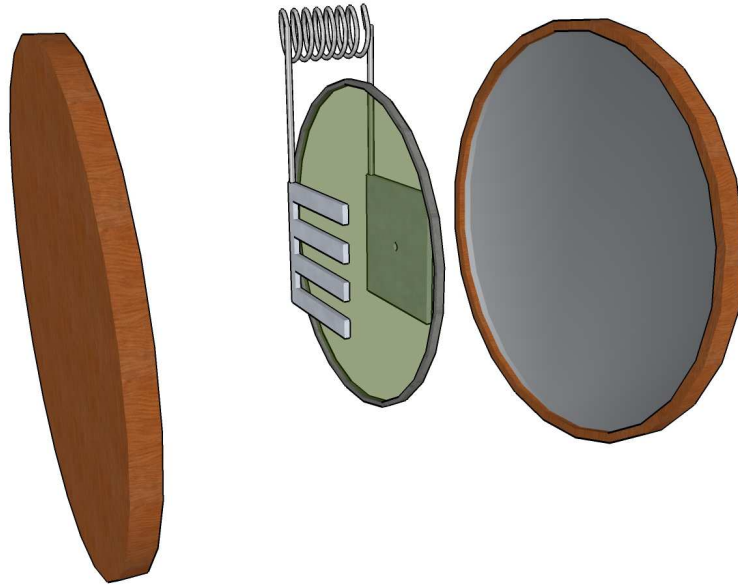


Figure 3: Cavity with a nanomechanical membrane, coupled to an LC-circuit.

2 Fundamentals

In order to analyze the coupled system which we introduced in the previous section, we need a technical approach to the question. The simple time delay description demonstrated that we have a damped harmonic oscillator for a red-detuned laser, thus, our goal is to develop a quantum mechanical description of dissipation.

Our starting point is the harmonic oscillator Hamiltonian

$$H = \frac{p^2}{2m} + \frac{1}{2}m\omega^2q^2 \quad (2)$$

and the equations of motion are

$$\begin{aligned} \dot{p} &= -\frac{\partial H}{\partial q} = -m\omega^2q \\ \dot{q} &= \frac{\partial H}{\partial p} = \frac{p}{m} \end{aligned}$$

Classically, we can introduce damping into our system simply by adding a velocity dependent term,

$$\dot{p} = -\gamma p - m\omega^2q \quad (3)$$

where $\gamma > 0$.

The question is whether this simple approach can be transferred directly to quantum mechanics. The Heisenberg equations of motion are exactly the same for the quantized harmonic oscillator, so all that is left to do is to replace the generalized position and momentum with the corresponding operators, \hat{q} and \hat{p} . In contrast to classical mechanics, the position and momentum operators do not commute, and we have the well-known canonical commutation relation

$$[\hat{q}, \hat{p}] = i\hbar \quad (4)$$

Now, let us consider the time evolution of the commutator, using the equations of motion

$$\begin{aligned} \frac{d}{dt} [\hat{q}, \hat{p}] &= \dot{\hat{q}}\hat{p} + \hat{q}\dot{\hat{p}} - \dot{\hat{p}}\hat{q} - \hat{p}\dot{\hat{q}} \\ &= \frac{\hat{p}^2}{m} - \hat{q}(\gamma\hat{p} + m\omega^2\hat{q}) + (\gamma\hat{p} + m\omega^2\hat{q})\hat{q} - \frac{\hat{p}^2}{m} \\ &= -\gamma [\hat{q}, \hat{p}] \end{aligned}$$

By formal integration we arrive at the following result

$$[\hat{q}(t), \hat{p}(t)] = e^{-\gamma t} [\hat{q}(0), \hat{p}(0)] \quad (5)$$

As we can see, the commutator decays in time, and, although the ad hoc approach seemed reasonable, the description is inadequate. So the question is how we can introduce dissipation while preserving the commutator relation.

2.1 Brownian motion and classical Langevin equation

In order to understand why this approach is incomplete, we should consider the following example. Let us imagine a pendulum submerged in a viscous fluid. We assume that the massive object at the end of the rod has higher density than the fluid, thus the object will oscillate around the equilibrium position. The oscillator is obviously damped and at some point it will come to rest - at least, macroscopically. On the microscopic level, the massive object will constantly be bombarded by the surrounding molecules and, despite the fact that the contribution from the random momentum kicks is zero on average, the object will never entirely come to rest. This example illustrates the basic idea behind the so-called *fluctuation-dissipation theorem*. One could say that these two quantities, fluctuation and dissipation, come hand in hand. Furthermore, this example illustrates the concept of system-bath interaction, where a "system" with few degrees of freedom is brought in contact with a "heat bath" with many degrees of freedom.

The random movement of the pendulum at "rest" is also known as *Brownian motion* and was first observed by the botanist Robert Brown in the beginning of 19th century. Mathematically Brownian motion can be described by the *Langevin equation*, which reads [4, p.42]

$$m\ddot{x} = -V'(x) - \gamma\dot{x} + \sqrt{2\gamma kT}\xi(t) \quad (6)$$

where $V(x)$ is a potential field and $\xi(t)$ describes the fluctuating force. We seek to find an analogous equation for quantum systems, but before doing so, let us once again have a look at the concept of Brownian motion and how it relates to our work.

Once again we consider the simple optomechanical setup presented earlier. We think of the cavity as our "system" and the world outside (the environment) as the "heat bath"/reservoir - we say that the system is coupled to the reservoir. Since we have a lossy cavity, electromagnetic radiation can "leak out" from it. In a similar fashion, electromagnetic radiation can randomly leak into our cavity and disturb our system, which is basically equivalent to Brownian motion, where molecules randomly bump into a larger object. Let us consider a different example. If we drive our cavity with a red-detuned laser, the mechanical motion of the oscillator will be cooled. But although the motion is effectively being cooled, the average number of photons being scattered of the movable mirror fluctuates⁷. This resembles the random bombardement in the viscous fluid. Following these simple examples, one would conclude that a quantum mechanical analogue for the classical Langevin equation would provide one with appropriate quantum description of our optomechanical system.

2.2 Quantum theory of beam splitters

We will now briefly recall the basics of the quantum mechanical description of beam splitters. The purpose of this short intermezzo is to give the reader an alternative way to think of the system/reservoir picture. Let us begin with the well known illustration of a beam splitter (see Figure 4). The annihilation operators of the fields satisfy the bosonic

⁷The relative fluctuation in the number of photons is also known as *shot noise*.

commutation relations

$$\begin{aligned} [\hat{a}_i, \hat{a}_j^\dagger] &= \delta_{ij} \\ [\hat{a}_i, \hat{a}_j] &= [\hat{a}_i^\dagger, \hat{a}_j^\dagger] = 0 \end{aligned}$$

Following a standard textbook example, we say that \hat{a}_0 is the vacuum field, while \hat{a}_1 is the incoming signal (e.g. a coherent state). If we place a mirror at the end of the third arm and regard the field operator \hat{a}_2 as loss, we can almost think of the setup as our cavity. As we can see, the beam splitter picture provides us with all relevant elements: fluctuations (noise input), input signal and loss.

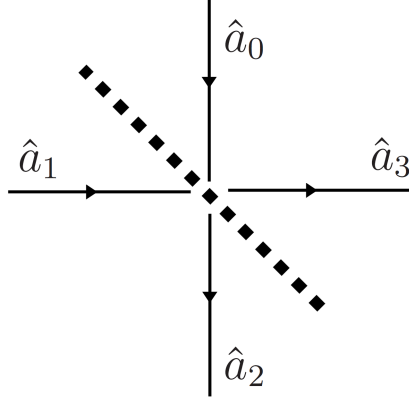


Figure 4: Quantum mechanical depiction of a beam splitter.

2.3 Quantum Langevin equation

Our approach towards constructing a quantum analogue to the Langevin equation will for now be purely phenomenological. Once again we consider the harmonic oscillator and, traditionally, the non-Hermitian *creation* and *annihilation* operators are introduced,

$$\hat{a} = \frac{\omega\hat{q} + i\hat{p}}{\sqrt{2\hbar\omega}} \quad \hat{a}^\dagger = \frac{\omega\hat{q}^\dagger - i\hat{p}^\dagger}{\sqrt{2\hbar\omega}} \quad (7)$$

satisfying the commutator relation $[\hat{a}, \hat{a}^\dagger] = 1$. As a result, the Hamiltonian takes the form,

$$\hat{H} = \hbar\omega \left(\hat{a}^\dagger \hat{a} + \frac{1}{2} \right) \quad (8)$$

and the Heisenberg equation of motion for the annihilation operator is

$$\dot{\hat{a}}(t) = \frac{i}{\hbar} [\hat{H}, \hat{a}] = -i\omega\hat{a}(t) \quad (9)$$

Taking the fluctuation-dissipation theorem into account, we now add a damping and a fluctuating term to the equation of motion

$$\dot{\hat{a}}(t) = -i\omega\hat{a}(t) - \gamma\hat{a}(t) + \sqrt{2\gamma}\hat{\xi}(t) \quad (10)$$

where γ is the damping rate and $\xi(t)$ is the fluctuating term. We can think of the latter as a *noise* input. The new equation of motion can be simplified by transforming to a rotating reference frame

$$\hat{A}(t) \equiv \hat{A}(t)e^{i\omega t} \quad (11)$$

$$(12)$$

where \hat{A} are the slowly varying operators (e.g. \hat{a} and $\hat{\xi}$). Thus the equation of motion in the rotating frame is

$$\dot{\hat{a}}(t) = -\gamma\hat{a}(t) + \sqrt{2\gamma}\hat{\xi}(t) \quad (13)$$

For convenience, we remove tildes from the new operators, yet keeping in mind that we are in a rotating frame.

Before solving the equation of motion, we assume that the noise operators are delta-correlated

$$[\hat{\xi}(t), \hat{\xi}^\dagger(t')] = D\delta(t - t') \quad (14)$$

$$\langle \hat{\xi}^\dagger(t)\hat{\xi}(t') \rangle = N\delta(t - t') \quad (15)$$

where the constants D and N remain to be determined. Now let us consider whether our assumption is reasonable. Eq. (14) corresponds to assuming that random forces at different times have nothing to do with each other - they are uncorrelated. The delta-correlation also assumes that the collision-time is very short.

We are now ready to solve the equation of motion by formal intergration

$$\begin{aligned} \dot{\hat{a}}(t)e^{\gamma t} &= -\gamma\hat{a}(t)e^{\gamma t} + \sqrt{2\gamma}\hat{\xi}(t)e^{\gamma t} \\ \frac{d}{dt} [\hat{a}(t)e^{\gamma t}] &= \sqrt{2\gamma}\hat{\xi}(t)e^{\gamma t} \\ \hat{a}(t) &= \hat{a}(0)e^{-\gamma t} + \sqrt{2\gamma} \int_0^t \hat{\xi}(t')e^{-\gamma(t-t')} dt' \end{aligned} \quad (16)$$

$$\hat{a}^\dagger(t) = \hat{a}^\dagger(0)e^{-\gamma t} + \sqrt{2\gamma} \int_0^t \hat{\xi}^\dagger(t'')e^{-\gamma(t-t'')} dt'' \quad (17)$$

First and foremost, we have to ensure that the commutation relation for the creation and annihilation operators are satisfied at all times

$$\begin{aligned} [\hat{a}(t), \hat{a}^\dagger(t)] &= [\hat{a}(0), \hat{a}^\dagger(0)] e^{-2\gamma t} + \sqrt{2\gamma} \int_0^t [\hat{a}(0), \hat{\xi}^\dagger(t'')] e^{-\gamma(2t-t'')} dt'' \\ &\quad - \sqrt{2\gamma} \int_0^t [\hat{a}^\dagger(0), \hat{\xi}(t')] e^{-\gamma(2t-t')} dt' \\ &\quad + 2\gamma \int_0^t \int_0^t [\hat{\xi}(t'), \hat{\xi}^\dagger(t'')] e^{-\gamma(2t-t'-t'')} dt' dt'' \end{aligned}$$

Assuming the commutation relations⁸

$$[\hat{a}(0), \hat{\xi}^\dagger(t)] = [\hat{a}^\dagger(0), \hat{\xi}(t)] = 0 \quad (18)$$

⁸In the beam-splitter analogy, this corresponds to the commutator of two different input fields (e.g. \hat{a}_0 and \hat{a}_1).

we arrive at the following result

$$\begin{aligned}
[\hat{a}(t), \hat{a}^\dagger(t)] &= e^{-2\gamma t} + 2\gamma D \int_0^t \int_0^t \delta(t' - t'') e^{-\gamma(2t-t'-t'')} dt' dt'' \\
&= e^{-2\gamma t} + 2\gamma D \int_0^t e^{-2\gamma(t-t')} dt' \\
&= e^{-2\gamma t} + D (1 - e^{-2\gamma t})
\end{aligned} \tag{19}$$

Thus the commutator of the annihilation operators are satisfied at all times for $D = 1$. So far our phenomenological approach seems to satisfy our requirements. In order to determine the constant N in eq. (14), we must consider the mean occupation number

$$\begin{aligned}
\langle \hat{a}^\dagger(t) \hat{a}(t) \rangle &= \langle \hat{a}^\dagger(0) \hat{a}(0) \rangle e^{-2\gamma t} \\
&\quad + 2\gamma \int_0^t \int_0^t \langle \hat{\xi}^\dagger(t'') \hat{\xi}(t') \rangle e^{-\gamma(2t-t'-t'')} dt' dt'' \\
&= N_0 e^{-2\gamma t} + N (1 - e^{-2\gamma t})
\end{aligned} \tag{20}$$

where N_0 is the occupation number of our harmonic oscillator at the initial time. This result is in fact very interesting and can be regarded as yet another manifestation of the fluctuation-dissipation theorem. At time $t = 0$, the mean occupation number is N_0 , as it should naturally be. But as time progresses, the contribution from N_0 decreases along with an increase in the contribution from N . If we let $t \rightarrow \infty$, the system and the reservoir will be in thermal equilibrium. And since the population of the system in thermal equilibrium equals the occupation number of the reservoir, the constant N is the occupation number of the reservoir at the initial time. This illustrates that due to the fact that our system interacts with the reservoir, there is dissipation (the first term in (19)) and at the same time excitations from the reservoir leak into our system - the "fluctuation" term.

As we can see, we have managed to construct an analogue to the classical Langevin equation that is consistent with quantum mechanics using some rather simple assumptions. The downside of this approach is unfortunately that our model might not be as transparent as we would like it to be, meaning that we might not be able to recognize the limitations. Therefore, we will provide a very brief overview of the formal derivation of quantum Langevin equation following the approach of C.W.Gardiner and M.J.Collett[5]. The foundation of the quantum damping theory developed by Gardiner and Collett are the following assumptions

- the system/bath interactions are linear in the bath operators
- the rotating-wave approximation is applied to the interaction Hamiltonian
- the coupling of the system to bath is independent of frequency, and the bath spectrum is assumed flat

Nonlinear interactions can occur if the fluctuations are rather large. This can be avoided by making sure that the cavity, membrane and the LC-circuit have a high- Q factor. Given advances in optomechanics in recent years, it is safe to assume a high quality factor for

the different components in our setup. Q -factors of the order $10^6 - 10^7$ [6] for the cavity and membrane are not unusual, while for the numbers the LC-circuit are of the order 10^2 . By assuming high- Q factors, hence weak-coupling to the reservoir, it is also safe to apply the rotating-wave approximation (more on that later). Finally, we consider the "flat spectrum" assumption. A flat spectrum corresponds to saying that all the different frequencies are present in equal amounts, which is also known as white noise.

The reservoir is modeled as a large ensemble of independent harmonic oscillators, which is rather reasonable in our case. Quantization of the electromagnetic field and elastic waves can be shown to be exactly equivalent to such an ensemble of oscillators.

It is assumed that the modes are very close to each other and the spectrum is approximated as a continuum. And finally, Gardiner and Collett introduce the *first Markov approximation*, which assumes a frequency independent coupling constant. These approximations significantly simplify the quantum Langevin equation, which ends up taking the same form as eq. (10).

Convinced that our phenomenological approach has in fact produced a reasonable description of quantum damping, we are almost ready to analyse our system.

2.4 Fourier analysis

In our analysis, the equations of motion will be very similar to (12), namely first-order ordinary differential equations. They will be solved using Fourier analysis.

In physics, we usually describe a sinusoidal wave travelling in the positive direction (in this case positive x -direction) as follows

$$f(x, t) = A \sin(kx - \omega t)$$

where A is the amplitude, k is the wave vector and ω is the angular frequency. In accordance with this convention, we define our Fourier transform as following⁹

$$\mathcal{F}[f(t)] \equiv \frac{1}{\sqrt{2\pi}} \int_{-\infty}^{\infty} f(t) e^{i\omega t} dt \quad (21)$$

Consequently, the inverse Fourier transform is

$$\mathcal{F}^{-1}[f(\omega)] = \frac{1}{\sqrt{2\pi}} \int_{-\infty}^{\infty} f(\omega) e^{-i\omega t} d\omega$$

Finally, we recall one last important result from Fourier analysis, namely, the Fourier transform representation of the δ -function

$$\delta(t - s) = \frac{1}{2\pi} \int_{-\infty}^{\infty} e^{-i\omega(t-s)} d\omega \quad (22)$$

This expression can be shown to be true using the Fourier inversion theorem [7, p.442].

⁹The space-time transform is respectively $f(\mathbf{x}, t) = (2\pi)^{-3/2} \int_{-\infty}^{\infty} \int_{-\infty}^{\infty} \int_{-\infty}^{\infty} f(\mathbf{k}, \omega) e^{i(\mathbf{k}\cdot\mathbf{x} - \omega t)} d\mathbf{k} d\omega$.

3 Analysis I: weak-coupling regime

We are finally ready to analyse the setup, presented at the beginning of this thesis (see Figure 3). Following up on the discussion on system/reservoir interaction in the previous section, we consider the following illustration, providing an overview of the total system and reservoir

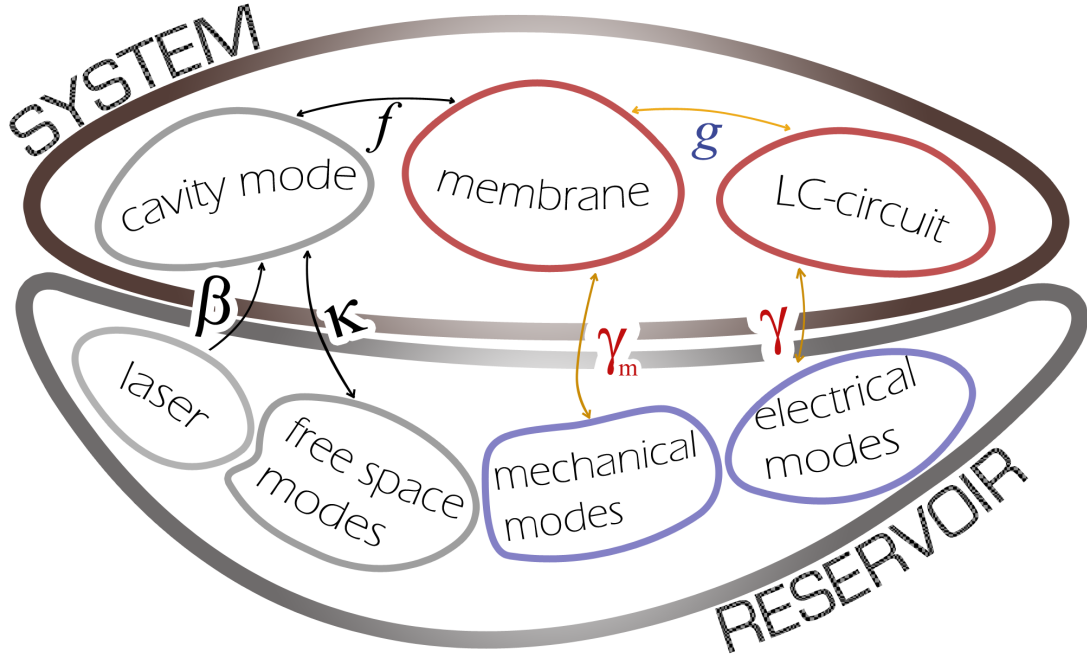


Figure 5: An illustration of the system-reservoir division.

The arrows indicate decay into a reservoir/noise input and couplings between the sub-components of the total system. As indicated, we assume no interaction between the reservoirs, which should be possible to realise experimentally.

Our analysis will only deal with the coupling of membrane to the LC-circuit and the interaction of these components with the respective reservoirs (the coloured part of the illustration). The full Hamiltonian in natural units (e.g. $\hbar = 1$) is given by [1]

$$\hat{H} = \omega_m \hat{a}^\dagger \hat{a} + \omega_0 \hat{b}^\dagger \hat{b} + \frac{g}{2} (\hat{a} + \hat{a}^\dagger) (\hat{b} + \hat{b}^\dagger) \quad (23)$$

where \hat{a} and \hat{b} are the annihilation operators for the membrane and the LC-circuit, respectively. The coupling constant g is assumed to be real. Our analysis will only be concerned with on-resonant case (e.g. $\omega_m = \omega_0 = \omega$).

The equations of motion for the annihilation operators are

$$\begin{aligned} \dot{\hat{a}} &= i [\hat{H}, \hat{a}] = -i\omega \hat{a} - i\frac{g}{2} (\hat{b} + \hat{b}^\dagger) \\ \dot{\hat{b}} &= i [\hat{H}, \hat{b}] = -i\omega \hat{b} - i\frac{g}{2} (\hat{a} + \hat{a}^\dagger) \end{aligned}$$

3.1 The rotating-wave approximation

Similar to our approach in the previous section, we transform to a rotating frame by introducing fast varying operators (see eq. (11)). We consider the equation of motion for the membrane annihilation operator

$$\begin{aligned}\dot{\hat{a}} &= -i\frac{g}{2}(\hat{b}e^{i\omega t} + \hat{b}^\dagger e^{i\omega t}) \\ &= -i\frac{g}{2}(\hat{\tilde{b}} + \hat{\tilde{b}}^\dagger e^{2i\omega t})\end{aligned}$$

where in the last line we have used that $\hat{b}^\dagger = \hat{\tilde{b}}e^{-i\omega t}$ (following eq. (11)). Assuming weak-coupling regime (e.g. $g \ll \omega$), the rapidly varying term can be disregarded, since its contribution to the average is negligible. In terms of the Hamiltonian, this corresponds to neglecting the cross terms (e.g. $\hat{a}\hat{\tilde{b}}$ and $\hat{a}^\dagger\hat{\tilde{b}}^\dagger$), meaning that we are only interested in processes where one quantum of energy in the membrane is annihilated, while an energy quantum is created in the LC-circuit, and vice versa.

Once again we remove tildes for convenience. Hence the equations of motion in the rotating frame and rotating-wave approximation (along with damping and noise taken into account) take the form

$$\begin{aligned}\dot{\hat{a}} &= -\gamma_m\hat{a} + \sqrt{2\gamma_m}\hat{a}_{in} - i\frac{g}{2}\hat{b} \\ \dot{\hat{b}} &= -\gamma\hat{b} + \sqrt{2\gamma}\hat{b}_{in} - i\frac{g}{2}\hat{a}\end{aligned}\tag{24}$$

Here, γ_m is the intrinsic damping rate of the membrane, but since we are interested in cooling the motion of the membrane by radiation pressure, γ_m is replaced by an effective damping rate Γ_m

$$\dot{\hat{a}} = -\Gamma_m\hat{a} + \sqrt{2\gamma_m}\hat{a}_{in} - i\frac{g}{2}\hat{b}\tag{25}$$

Eqs. (24) and (25) are the quantum Langevin equations (also referred to as *Heisenberg-Langevin* equations) that we will look at.

3.2 Simple limiting cases

In order to gain a physical understanding of the system involved, we begin with a derivation and discussion of the simple limits presented in [1]. The limits in question are the strong- and weak-damping limits (e.g. $g \ll \Gamma_m$ and $g \gg \Gamma_m$).

One can think of our system as two pendula connected with a spring. The spring constant corresponds to the coupling constant g in our setup. Damping of the membrane and the LC-circuit can be introduced into this simple picture if we imagine that the pendula as submerged in two different viscous fluids (while the spring, coupling the pendula, is unaffected by this). This analogy can be used to gain an understanding of the physics.

First, we consider the strong-damping limit where $\Gamma_m \gg g, \gamma$. In this limit the strongly damped oscillator (e.g. the membrane) rapidly relaxes to a quasi-stationary state (on a time scale Γ_m^{-1}) and, thereafter, follows the evolution of the second oscillator (e.g. the

LC-circuit). This is essentially the idea behind a technique called *adiabatic elimination* - "long-living systems slave short-living systems" [8]. In our case, the LC-circuit is the "long-living system" (i.e. $\Gamma_m^{-1} \ll \gamma^{-1}$), meaning that we can adiabatically eliminate the membrane degree of freedom. Mathematically this can be done by setting $\dot{\hat{a}} = 0$ (e.g. the variation of \hat{a} on a time scale $\sim \gamma^{-1}$ is negligible)

$$0 = -\Gamma_m \hat{a} + \sqrt{2\gamma_m} \hat{a}_{in} - i\frac{g}{2} \hat{b} \quad \Leftrightarrow \quad \hat{a} = \frac{\sqrt{2\gamma_m}}{\Gamma_m} \hat{a}_{in} - i\frac{g}{2\Gamma_m} \hat{b}$$

We insert the latter equation into eq. (23) to obtain

$$\begin{aligned} \dot{\hat{b}} &= -\gamma \hat{b} + \sqrt{2\gamma} \hat{b}_{in} - i\frac{g}{2} \left(\frac{\sqrt{2\gamma_m}}{\Gamma_m} \hat{a}_{in} - i\frac{g}{2\Gamma_m} \hat{b} \right) \\ &= -(\gamma + \Gamma) \hat{b} + \sqrt{2\gamma} \hat{b}_{in} - i\frac{g}{2\Gamma_m} \sqrt{2\gamma_m} \hat{a}_{in} \end{aligned}$$

where $\Gamma \equiv g^2/4\Gamma_m$. By formal integration we obtain the following result

$$\begin{aligned} \hat{b}(t) &= \sqrt{2\gamma} \int_{-\infty}^t \hat{b}_{in}(t') e^{-(\gamma+\Gamma)(t-t')} dt' - i\frac{g}{2\Gamma_m} \sqrt{2\gamma_m} \int_{-\infty}^t \hat{a}_{in}(t') e^{-(\gamma+\Gamma)(t-t')} dt' \\ \hat{b}^\dagger(t) &= \sqrt{2\gamma} \int_{-\infty}^t \hat{b}_{in}^\dagger(t'') e^{-(\gamma+\Gamma)(t-t'')} dt'' + i\frac{g}{2\Gamma_m} \sqrt{2\gamma_m} \int_{-\infty}^t \hat{a}_{in}^\dagger(t'') e^{-(\gamma+\Gamma)(t-t'')} dt'' \end{aligned}$$

and, using that,

$$\begin{aligned} \langle \hat{b}_{in}^\dagger(t) \hat{a}_{in}(t') \rangle &= \langle \hat{a}_{in}^\dagger(t) \hat{b}_{in}(t') \rangle = 0 \\ \langle \hat{b}_{in}^\dagger(t) \hat{b}_{in}(t') \rangle &= n_b \delta(t-t') \\ \langle \hat{a}_{in}^\dagger(t) \hat{a}_{in}(t') \rangle &= n_a \delta(t-t') \end{aligned}$$

the mean occupation number of the LC-circuit is found

$$\begin{aligned} \langle \hat{b}^\dagger \hat{b} \rangle &= 2\gamma \int_{-\infty}^t \int_{-\infty}^t \langle \hat{b}_{in}^\dagger(t'') \hat{b}_{in}(t') \rangle e^{-(\gamma+\Gamma)(2t-t'-t'')} dt' dt'' \\ &\quad + \frac{g^2}{4\Gamma_m^2} 2\gamma_m \int_{-\infty}^t \int_{-\infty}^t \langle \hat{a}_{in}^\dagger(t'') \hat{a}_{in}(t') \rangle e^{-(\gamma+\Gamma)(2t-t'-t'')} dt' dt'' \\ &= 2\gamma n_b \int_{-\infty}^t e^{-2(\gamma+\Gamma)(t-t')} dt' + \frac{g^2}{4\Gamma_m^2} 2\gamma_m n_a \int_{-\infty}^t e^{-2(\gamma+\Gamma)(t-t')} dt' \\ &= \frac{\gamma}{\gamma + \Gamma} n_b + \frac{g^2}{4\Gamma_m^2} \frac{\gamma_m}{\gamma + \Gamma} n_a \end{aligned} \tag{26}$$

We recall that the Q -factor of the membrane is significantly larger than the one of the LC-circuit (see section 2.3), hence $\gamma_m \ll \gamma$, and we disregard the last term for now. Thus, the relative occupation number is approximately $\gamma/(\gamma + \Gamma)$ and is minimised for Γ_m as small as possible¹⁰. However, this calculation was done in the strong-damping limit $\Gamma_m \gg g$ and thus it is not valid for small values of Γ_m compared to g .

¹⁰Recall that $\Gamma \equiv g^2/4\Gamma_m$.

This brings us to the other simple limit, namely, the weak-damping limit ($g \gg \Gamma_m$). In the pendula analogy, which we introduced in the beginning of this section, this corresponds to having a spring with a very large spring constant. The two pendula move "in sync", and, therefore we consider their collective motion. Quantum mechanically this corresponds to the *dressed state picture*, where instead of considering \hat{a} and \hat{b} separately we consider the evolution of their collective symmetric and anti-symmetric modes

$$\dot{\hat{a}} \pm \dot{\hat{b}} = \mp i \frac{g}{2} (\hat{a} \pm \hat{b}) - \frac{\Gamma_m + \gamma}{2} (\hat{a} \pm \hat{b}) - \frac{\Gamma_m - \gamma}{2} (\hat{a} \mp \hat{b}) + \sqrt{2\gamma_m} \hat{a}_{in} \pm \sqrt{2\gamma} \hat{b}_{in}$$

We introduce the combined operators $\hat{S}_{\pm} \equiv \hat{a} \pm \hat{b}$ and transform to a rotating frame with respect to the *dressed states*

$$\hat{\hat{S}}_{\pm} \equiv \hat{S}_{\pm} e^{\pm i g t / 2}$$

The noise operators are redefined as

$$\hat{\hat{a}}_{in} \equiv \hat{a}_{in} e^{\pm i g t / 2}$$

where the sign of the exponent depends on whether we are working with the symmetric- or antisymmetric modes. The derivation for $\hat{\hat{S}}_+$ is shown explicitly below

$$\begin{aligned} \dot{\hat{\hat{S}}}_+ &= \dot{\hat{S}}_+ e^{i g t / 2} + i \frac{g}{2} \hat{S}_+ e^{i g t / 2} \Leftrightarrow \dot{\hat{\hat{S}}}_+ = \dot{\hat{S}}_+ e^{-i g t / 2} - i \frac{g}{2} \hat{S}_+ \\ \dot{\hat{\hat{S}}}_+ e^{-i g t / 2} - i \frac{g}{2} \hat{S}_+ &= -i \frac{g}{2} \hat{S}_+ - \frac{\Gamma_m + \gamma}{2} \hat{S}_+ - \frac{\Gamma_m - \gamma}{2} \hat{S}_- + \sqrt{2\gamma_m} \hat{a}_{in} + \sqrt{2\gamma} \hat{b}_{in} \\ \dot{\hat{\hat{S}}}_+ &= -\frac{\Gamma_m + \gamma}{2} \hat{S}_+ - \frac{\Gamma_m - \gamma}{2} \hat{S}_- e^{i g t} + \sqrt{2\gamma_m} \hat{a}_{in} + \sqrt{2\gamma} \hat{b}_{in} \\ &\approx -\frac{\Gamma_m + \gamma}{2} \hat{\hat{S}}_+ + \sqrt{2\gamma_m} \hat{\hat{a}}_{in} + \sqrt{2\gamma} \hat{\hat{b}}_{in} \end{aligned} \quad (27)$$

where we have used the rotating wave approximation in the last step. As we can see the damping rate of the $\hat{\hat{S}}_+$ mode is the average of the two damping rates Γ_m and γ . In a similar fashion one can show that the equation of motion for the $\hat{\hat{S}}_-$ mode is

$$\dot{\hat{\hat{S}}}_- = -\frac{\Gamma_m + \gamma}{2} \hat{\hat{S}}_- + \sqrt{2\gamma_m} \hat{\hat{a}}_{in} - \sqrt{2\gamma} \hat{\hat{b}}_{in} \quad (28)$$

We solve these equations of motion by formally integrating eqs. (26) and (27)

$$\hat{\hat{S}}_{\pm} = \sqrt{2\gamma_m} \int_{-\infty}^t \hat{\hat{a}}_{in}(t') e^{-(\Gamma_m + \gamma)(t-t')/2} dt' \pm \sqrt{2\gamma} \int_{-\infty}^t \hat{\hat{b}}_{in}(t') e^{-(\Gamma_m + \gamma)(t-t')/2} dt' \quad (29)$$

Now, we wish to find the total occupation number of our system (e.g. membrane and LC-circuit), which can be done in the following way

$$\begin{aligned} \frac{1}{2} \left\langle \hat{\hat{S}}_+^\dagger \hat{\hat{S}}_+ + \hat{\hat{S}}_-^\dagger \hat{\hat{S}}_- \right\rangle &= \langle \hat{a}^\dagger \hat{a} + \hat{b}^\dagger \hat{b} \rangle \\ &= 2\gamma_m \int_{-\infty}^t \int_{-\infty}^t \langle \hat{\hat{a}}_{in}^\dagger(t'') \hat{\hat{a}}_{in}(t') \rangle e^{-(\Gamma_m + \gamma)(2t-t'-t'')/2} dt' dt'' \\ &\quad + 2\gamma \int_{-\infty}^t \int_{-\infty}^t \langle \hat{\hat{b}}_{in}^\dagger(t'') \hat{\hat{b}}_{in}(t') \rangle e^{-(\Gamma_m + \gamma)(2t-t'-t'')/2} dt' dt'' \\ &= 2\gamma_m n_a \int_{-\infty}^t e^{-(\Gamma_m + \gamma)(t-t')} dt' + 2\gamma n_b \int_{-\infty}^t e^{-(\Gamma_m + \gamma)(t-t')} dt' \\ &= \frac{2\gamma_m}{\Gamma_m + \gamma} n_a + \frac{2\gamma}{\Gamma_m + \gamma} n_b \end{aligned}$$

Due to the fact that we are in the strong-coupling/weak-damping regime, the total occupation number is distributed equally between the membrane and the LC-circuit. Therefore, the occupation number of the LC is

$$\frac{\gamma_m}{\Gamma_m + \gamma} n_a + \frac{\gamma}{\Gamma_m + \gamma} n_b \quad (30)$$

where the first term can once again be ignored, and, thus, the relative occupation number is approximately $\gamma/(\Gamma_m + \gamma)$. In order to achieve the lowest possible number of excitations, Γ_m has to be as large as possible - while satisfying $\Gamma_m \ll g$, which draws the limit, within which this calculation can be valid.

The illustration below combines our results from the strong- and weak-damping limits

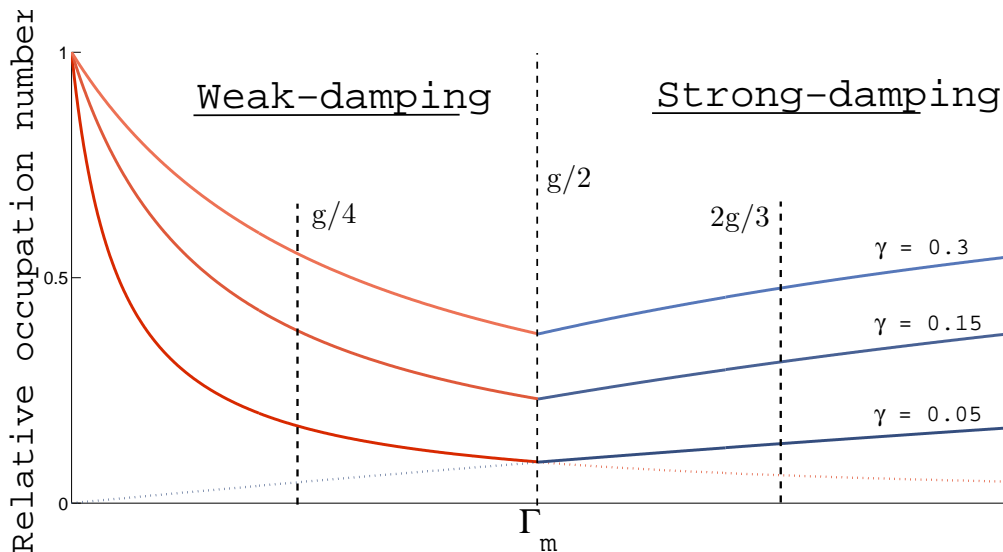


Figure 6: The relative occupation number of the LC-circuit $\langle \hat{b}^\dagger \hat{b} \rangle / n_b$ for different values of γ in the strong- and weak-damping limits.

One can clearly see from the expressions derived, that the minimum occupation number is achieved for $\Gamma_m = g/2$. Furthermore, it is obviously desirable to have a small intrinsic damping rate for the LC-circuit (e.g. a high- Q LC-circuit).

Now that we have understood the physics in the two simple limits, we are ready to find the full solution for the Heisenberg-Langevin equations for our system. We put to find a higher relative occupation number for $\Gamma_m = g/2$, but the question is how much higher.

3.3 Full derivation

So far we have been solving our equations of motion in the time-domain. However, solving the equations in the frequency-domain (e.g. Fourier-space) is in fact slightly easier in our case.

First, we write down our equations of motion in vector form

$$\underbrace{\begin{pmatrix} \dot{\hat{a}} \\ \dot{\hat{b}} \end{pmatrix}}_{\dot{\hat{V}}} = \underbrace{\begin{pmatrix} -\Gamma_m & -i\frac{g}{2} \\ -i\frac{g}{2} & \gamma \end{pmatrix}}_{\tilde{\mathbf{M}}} \underbrace{\begin{pmatrix} \hat{a} \\ \hat{b} \end{pmatrix}}_{\hat{V}} + \underbrace{\begin{pmatrix} \sqrt{2\gamma_m} \hat{a}_{in} \\ \sqrt{2\gamma} \hat{b}_{in} \end{pmatrix}}_{\tilde{\mathbf{F}}} \quad (31)$$

Following our definition of the Fourier transform in section 2.4 (see eq. (20)), it can be easily shown (by integration by parts) that

$$\mathcal{F}[f'(t)] = -i\omega\mathcal{F}[f(t)] \quad (32)$$

We Fourier transform eq. (29)

$$\begin{aligned} -i\omega\bar{V}(\omega) &= \tilde{\mathbf{M}}(\omega)\bar{V}(\omega) + \bar{F}(\omega) \\ \underbrace{(-\tilde{\mathbf{M}}(\omega) - i\omega\mathbf{I})}_{\mathbf{M}}\bar{V}(\omega) &= \bar{F}(\omega) \\ \bar{V}(\omega) &= \mathbf{M}^{-1}\bar{F}(\omega) \end{aligned}$$

where \mathbf{I} is the identity matrix. Therefore, the first step to be taken is inverting the matrix \mathbf{M} , which can be done using standard inversion schemes ¹¹

$$\mathbf{M}^{-1} = \frac{1}{\mathcal{D}(\omega)} \begin{pmatrix} \gamma - i\omega & -i\frac{g}{2} \\ -i\frac{g}{2} & \Gamma_m - i\omega \end{pmatrix} \quad (33)$$

where $\mathcal{D}(\omega)$ is the determinant of the matrix \mathbf{M}

$$\mathcal{D}(\omega) = (\Gamma_m - i\omega)(\gamma - i\omega) + \frac{g^2}{4} \quad (34)$$

The annihilation operator (in frequency-domain) for the LC is therefore

$$\hat{b}(\omega) = -\frac{i}{2}\frac{g}{\mathcal{D}(\omega)}\sqrt{2\gamma_m}\hat{a}_{in}(\omega) + \frac{\Gamma_m - i\omega}{\mathcal{D}(\omega)}\sqrt{2\gamma}\hat{b}_{in}(\omega)$$

Before proceeding, we find the correlation functions for the noise operators in Fourier-space

$$\begin{aligned} \hat{a}(\omega') &= \frac{1}{\sqrt{2\pi}} \int_{-\infty}^{\infty} \hat{a}_{in}(t') e^{i\omega't'} dt' \\ \hat{a}^\dagger(\omega) &= \frac{1}{\sqrt{2\pi}} \int_{-\infty}^{\infty} \hat{a}_{in}^\dagger(t) e^{-i\omega t} dt \\ \langle \hat{a}^\dagger(\omega) \hat{a}(\omega') \rangle &= \frac{1}{2\pi} \int_{-\infty}^{\infty} \int_{-\infty}^{\infty} \langle \hat{a}_{in}^\dagger(t) \hat{a}_{in}(t') \rangle e^{-i\omega t + i\omega' t'} dt dt' \\ &= \frac{1}{2\pi} n_a \int_{-\infty}^{\infty} \int_{-\infty}^{\infty} \delta(t - t') e^{-i\omega t + i\omega' t'} dt dt' \\ &= \frac{1}{2\pi} n_a \int_{-\infty}^{\infty} e^{-i(\omega - \omega')t} dt \\ &= n_a \delta(\omega - \omega') \end{aligned} \quad (35)$$

where we have used eq. (21) in the last step. As we can see, the correlation functions for the noise operators in frequency-domain are "identical" to those in the time-domain.

By inverse Fourier transformation, we obtain the following expression for \hat{b}

$$\hat{b}(t) = -i\frac{g}{2}\sqrt{\frac{2\gamma_m}{2\pi}} \int_{-\infty}^{\infty} \frac{1}{\mathcal{D}(\omega)} \hat{a}_{in}(\omega) e^{-i\omega t} d\omega + \sqrt{\frac{2\gamma}{2\pi}} \int_{-\infty}^{\infty} \frac{\Gamma_m - i\omega}{\mathcal{D}(\omega)} \hat{b}_{in}(\omega') e^{-i\omega t} d\omega$$

¹¹<http://www.cg.info.hiroshima-cu.ac.jp/~miyazaki/knowledge/teche23.html>

Consequently, the Hermitian conjugate is

$$\hat{b}^\dagger(t) = i\frac{g}{2}\sqrt{\frac{2\gamma_m}{2\pi}}\int_{-\infty}^{\infty}\frac{1}{\mathcal{D}^*(\omega')}\hat{a}_{in}^\dagger(\omega')e^{i\omega't}d\omega' + \sqrt{\frac{2\gamma}{2\pi}}\int_{-\infty}^{\infty}\frac{\Gamma_m + i\omega'}{\mathcal{D}^*(\omega')}\hat{b}_{in}^\dagger(\omega')e^{i\omega't}d\omega'$$

Thus, the mean occupation number is

$$\begin{aligned}\langle\hat{b}^\dagger\hat{b}\rangle &= \frac{g^2}{4}\frac{2\gamma_m}{2\pi}\int_{-\infty}^{\infty}\int_{-\infty}^{\infty}\frac{1}{\mathcal{D}^*(\omega')\mathcal{D}(\omega)}\langle\hat{a}_{in}^\dagger(\omega')\hat{a}_{in}(\omega)\rangle e^{i(\omega'-\omega)t}d\omega'd\omega \\ &+ \frac{2\gamma}{2\pi}\int_{-\infty}^{\infty}\int_{-\infty}^{\infty}\frac{(\Gamma_m + i\omega')(\Gamma_m - i\omega)}{\mathcal{D}^*(\omega')\mathcal{D}(\omega)}\langle\hat{b}_{in}^\dagger(\omega')\hat{b}_{in}(\omega)\rangle e^{i(\omega'-\omega)t}d\omega'd\omega \\ &= \frac{g^2}{4}\frac{2\gamma_m}{2\pi}n_a\int_{-\infty}^{\infty}\frac{1}{\mathcal{D}^*(\omega)\mathcal{D}(\omega)}d\omega + \frac{2\gamma}{2\pi}n_b\int_{-\infty}^{\infty}\frac{\Gamma_m^2 + \omega^2}{\mathcal{D}^*(\omega)\mathcal{D}(\omega)}d\omega\end{aligned}$$

We evaluate these integrals through the method of *contour integration* (integration in the complex plane). First, we find the poles (e.g. singularities of the integrands). This corresponds to solving $\mathcal{D}(\omega) = 0$ for ω

$$\omega = -i\frac{\Gamma_m + \gamma}{2} \pm \frac{1}{2}\sqrt{g^2 - (\Gamma_m - \gamma)^2} \quad (36)$$

Similarly, if we solved for $\mathcal{D}^*(\omega) = 0$, we would find the exact same poles, only in the upper half-plane.

The next step is to find the residues at the poles in the lower half-plane¹². Since we are working with simple poles, the residues for each of them can be found quite easily. Our integrands have a general form of $k(\omega)/h(\omega)$, thus, the residue at a given pole can be found as follows [7, p.858]

$$\mathcal{R}(\omega_j) = \frac{k(\omega_j)}{h'(\omega_j)} \quad (37)$$

and the integrals are evaluated by summing the residues

$$\int_{-\infty}^{\infty}\frac{k(\omega)}{h(\omega)}d\omega = 2\pi i\sum_j\mathcal{R}(\omega_j)$$

By doing so we arrive at the following expression for the occupation number¹³

$$\boxed{\langle\hat{b}^\dagger\hat{b}\rangle = \frac{\gamma_m g^2}{4\Gamma_m^2\gamma + 4\Gamma_m\gamma^2 + \Gamma_m g^2 + \gamma g^2}n_a + \frac{\gamma(4\Gamma_m^2 + 4\Gamma_m\gamma + g^2)}{4\Gamma_m^2\gamma + 4\Gamma_m\gamma^2 + \Gamma_m g^2 + \gamma g^2}n_b} \quad (38)$$

Although not as simple as the earlier expressions for the limiting cases, this expression is manageable. Let us start by comparing this result with the approximate expressions earlier considered (e.g. eqs. (25) and (29)). We assume approximately equal number of excitations initially in the reservoirs ($\bar{N} = n_a \approx n_b$).

The figure below illustrates how the exact solution approaches the limiting case solutions

¹²In our case this doesn't matter, since the poles are located symmetrically.

¹³Although this method of solving the integrals is fairly simple, the calculation of the residues is rather tedious and has no special significance for our work. Therefore the residues are found using **Maple**.

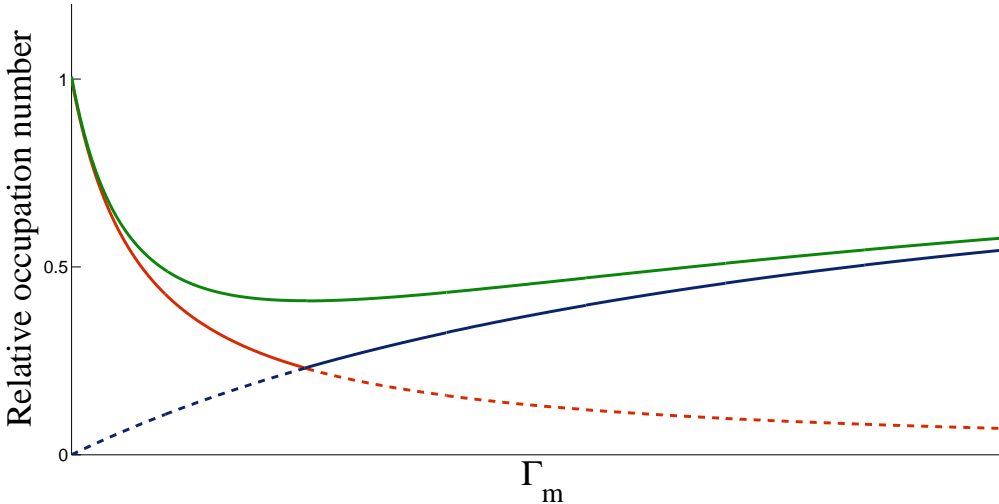


Figure 7: The exact relative occupation number of the LC-circuit $\langle \hat{b}^\dagger \hat{b} \rangle / \bar{N}$ compared with the limiting cases. Here $\gamma = 0.15 \text{ s}^{-1}$ and $\gamma_m = 10^{-3} \text{ s}^{-1}$. See Appendix A for more illustrations.

discussed in the previous section. Clearly, the minimum number of excitations in the LC-circuit is higher for a given set of damping rates, γ and γ_m than earlier expected. Furthermore, the optimal damping rate is slightly shifted with respect to $g/2$

$$\bar{\Gamma}_m = \gamma_m + \frac{g}{2} \sqrt{1 + \frac{4\gamma_m^2}{g^2} + \frac{4\gamma_m\gamma}{g^2} + \frac{\gamma_m}{\gamma}} \quad (39)$$

However, in the limit $g \gg \gamma_m, \gamma$ the optimal external damping rate is approximately $\bar{\Gamma}_m \approx g/2$. In the following, we assume this limit to be true and consider the minimum occupation number. From eqs. (25) and (29), we find that the number of excitations for an external damping rate $g/2$ is

$$\frac{\langle \hat{b}^\dagger \hat{b} \rangle}{\bar{N}} = \frac{2(\gamma_m + \gamma)}{2\gamma + g} \approx \frac{2\gamma}{g} \quad (40)$$

where we have once again used the fact that $\gamma \gg \gamma_m$. From the exact solution we find that the minimum occupation number is

$$\frac{\langle \hat{b}^\dagger \hat{b} \rangle}{\bar{N}} = \frac{2(\gamma_m g + 2\gamma g + 2\gamma^2)}{(2\gamma + g)^2} \approx \frac{4\gamma}{g} \quad (41)$$

As we can see there is approximately a factor of 2 difference between the minimum occupation number found in the simple limiting cases and the exact solution. This result shows once again that in order to achieve a low number of excitations in the LC-circuit, one must make sure to minimize the intrinsic damping rate γ and/or increase the coupling constant g .

Finally, we evaluate the occupation number at $\Gamma_m = g/2$ in the approximate and exact solutions, and consider the number of excitations as a function of the coupling constant

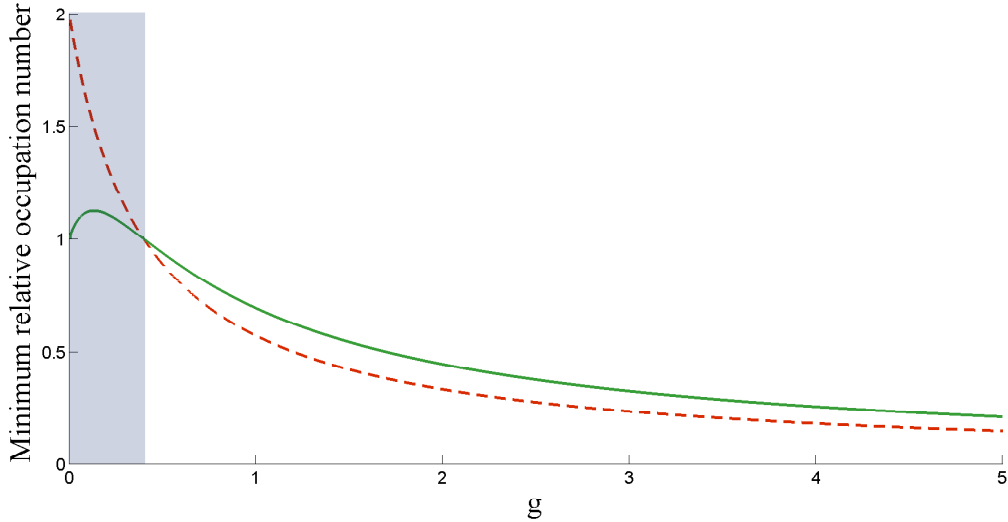


Figure 8: The minimum relative occupation number as a function of the coupling constant g . Here $\gamma = \gamma_m = 0.2 \text{ s}^{-1}$.

Clearly, the behaviour in the shaded region is somewhat strange. We find the intersection between the exact and approximate solutions to be at $g = 2\gamma_m$, corresponding to $\Gamma_m < \gamma_m$, which perfectly makes sense. After all, Γ_m is the effective damping - the combination of the intrinsic mechanical damping of the membrane, γ_m , and an external damping rate. Thus the physics is downright wrong for $\Gamma_m < \gamma_m$.

We have now analysed our coupled system and compared the exact solution with the approximate ones, with one of the main results being the lowest achievable number of excitations (see eq. (40)). However, our calculations are only accurate when the frequency of the membrane/LC-circuit is much larger than the coupling constant g . Thus we wish to find out when the rotating-wave approximation breaks down, which will be our motivation in the next section.

4 Analysis II: strong-coupling regime

The objective of this section is to find out when the rotating-wave approximation breaks down.

Our starting point is once again the Hamiltonian, which we presented in the beginning of the last section (see eq. (2)). Assuming the membrane being on-resonant with the LC-circuit ($\tilde{\omega} = \omega_m = \omega_0$), the equations of motion for the creation and annihilation operators (including damping and noise) are

$$\begin{aligned}\dot{\hat{a}} &= -i\tilde{\omega}\hat{a} - \Gamma_m\hat{a} + \sqrt{2\gamma_m}\hat{a}_{in} - i\frac{g}{2}(\hat{b} + \hat{b}^\dagger) \\ \dot{\hat{a}^\dagger} &= i\tilde{\omega}\hat{a}^\dagger - \Gamma_m\hat{a}^\dagger + \sqrt{2\gamma_m}\hat{a}_{in}^\dagger + i\frac{g}{2}(\hat{b} + \hat{b}^\dagger) \\ \dot{\hat{b}} &= -i\tilde{\omega}\hat{b} - \gamma\hat{b} + \sqrt{2\gamma}\hat{b}_{in} - i\frac{g}{2}(\hat{a} + \hat{a}^\dagger) \\ \dot{\hat{b}^\dagger} &= i\tilde{\omega}\hat{b}^\dagger - \gamma\hat{b}^\dagger + \sqrt{2\gamma}\hat{b}_{in}^\dagger + i\frac{g}{2}(\hat{b} + \hat{b}^\dagger)\end{aligned}$$

Once again we write the equations of motion in vector form

$$\underbrace{\begin{pmatrix} \dot{\hat{a}} \\ \dot{\hat{a}^\dagger} \\ \dot{\hat{b}} \\ \dot{\hat{b}^\dagger} \end{pmatrix}}_{\dot{\hat{V}}} = \underbrace{\begin{pmatrix} -\Gamma_m - i\tilde{\omega} & 0 & -i\frac{g}{2} & -i\frac{g}{2} \\ 0 & -\Gamma_m + i\tilde{\omega} & i\frac{g}{2} & i\frac{g}{2} \\ -i\frac{g}{2} & -i\frac{g}{2} & -\gamma - i\tilde{\omega} & 0 \\ i\frac{g}{2} & i\frac{g}{2} & 0 & -\gamma + i\tilde{\omega} \end{pmatrix}}_{\tilde{\mathbf{M}}} \underbrace{\begin{pmatrix} \hat{a} \\ \hat{a}^\dagger \\ \hat{b} \\ \hat{b}^\dagger \end{pmatrix}}_{\hat{V}} + \underbrace{\begin{pmatrix} \sqrt{2\gamma_m}\hat{a}_{in} \\ \sqrt{2\gamma_m}\hat{a}_{in}^\dagger \\ \sqrt{2\gamma}\hat{b}_{in} \\ \sqrt{2\gamma}\hat{b}_{in}^\dagger \end{pmatrix}}_{\tilde{F}}$$

and transform to Fourier-space

$$\begin{aligned}-i\omega\bar{V}(\omega) &= \tilde{\mathbf{M}}\bar{V}(\omega) + \tilde{F}(\omega) \\ \bar{V}(\omega) &= \mathbf{M}^{-1}\tilde{F}(\omega)\end{aligned}$$

where $\mathbf{M} = -\tilde{\mathbf{M}}(\omega) - i\omega\mathbf{I}$. Contrary the 2x2 matrix considered in the last section, the entries of the inverse \mathbf{M}^{-1} are rather large and space consuming. Therefore, we refer the reader to Appendix B for the complete inverted matrix. Here, we will mainly refer to the entries of \mathbf{M}^{-1} as $m_{i,j}$ (e.g. i -th row and j -th column). The determinant of \mathbf{M} is

$$\mathcal{D}(\omega) = (\Gamma_m + i\tilde{\omega} - i\omega)(\Gamma_m - i\tilde{\omega} - i\omega)(\gamma + i\tilde{\omega} - i\omega)(\gamma - i\tilde{\omega} - i\omega) - g^2\tilde{\omega}^2 \quad (42)$$

The creation and annihilation operators associated with the LC-circuit are

$$\begin{aligned}\hat{b}(\omega) &= \frac{\sqrt{2\gamma_m}m_{3,1}(\omega)\hat{a}_{in}(\omega) + \sqrt{2\gamma_m}m_{3,2}(\omega)\hat{a}_{in}^\dagger(\omega) + \sqrt{2\gamma}m_{3,3}(\omega)\hat{b}_{in}(\omega) + \sqrt{2\gamma}m_{3,4}(\omega)\hat{b}_{in}^\dagger(\omega)}{\mathcal{D}(\omega)} \\ \hat{b}^\dagger(\omega') &= \frac{\sqrt{2\gamma_m}m_{4,1}(\omega')\hat{a}_{in}(\omega') + \sqrt{2\gamma_m}m_{4,2}(\omega')\hat{a}_{in}^\dagger(\omega') + \sqrt{2\gamma}m_{4,3}(\omega')\hat{b}_{in}(\omega') + \sqrt{2\gamma}m_{4,4}(\omega')\hat{b}_{in}^\dagger(\omega')}{\mathcal{D}(\omega')}\end{aligned}$$

4.1 Looking at the general picture

Before doing inverse Fourier transformation, we have to consider a couple of details. Until now, we have done inverse Fourier transformation to find the annihilation operators in the time-domain. The creation operators were then simply the Hermitian conjugate of the annihilation operators (e.g. see at the top of p. 19). However, we are now supposed to invert a creation operator and thus have to be careful regarding the correlation functions. We define the inverse Fourier transform of a creation operator as following

$$\mathcal{F}^{-1} [\hat{a}^\dagger(\omega)] \equiv \frac{1}{\sqrt{2\pi}} \int_{-\infty}^{\infty} \hat{a}^\dagger(\omega) e^{-i\omega t} d\omega \quad (43)$$

Following this convention one can easily illustrate (similar to the calculations leading up to eq. (34)) that the correlation function for the noise operators is now

$$\langle \hat{a}_{in}^\dagger(\omega) \hat{a}_{in}(\omega') \rangle = n_a \delta(\omega + \omega') \quad (44)$$

$$\langle \hat{a}_{in}(\omega) \hat{a}_{in}^\dagger(\omega') \rangle = (n_a + 1) \delta(\omega + \omega') \quad (45)$$

where the last correlation function has been found using the bosonic commutator relation.

Now, let us once again consider Figure 5, showing the various reservoirs. There is one single detail in this illustration that we have yet to take into account: namely, the fact that there is also a coupling between the membrane and the laser-reservoir. This means that we have to consider an extra noise term $\sqrt{2(\Gamma_m - \gamma_m)} \hat{a}_{in}$, where $\Gamma_m - \gamma_m$ is the damping rate due to vacuum fluctuations. But does this mean that the calculations in the previous section are wrong?

Luckily, the answer to this question is "no". In order to see why, let us consider the following "effective" noise operator

$$\sqrt{2\gamma_m} \hat{a}_{in} = \sqrt{2\gamma_m} \hat{a}_{in} + \sqrt{2(\Gamma_m - \gamma_m)} \hat{a}_{in} \quad (46)$$

We find the occupation number to be

$$\begin{aligned} 2\gamma_m \langle \hat{a}_{in}^\dagger(t) \hat{a}_{in}(t') \rangle &= 2\gamma_m \langle \hat{a}_{in}^\dagger(t) \hat{a}_{in}(t') \rangle + 2(\Gamma_m - \gamma_m) \langle \hat{a}_{in}^\dagger(t) \hat{a}_{in}(t') \rangle \\ 2\gamma_m n_a \delta(t - t') &= 2\gamma_m \bar{n}_a \delta(t - t') + 2(\Gamma_m - \gamma_m) \bar{n}_a \delta(t - t') \end{aligned}$$

where \bar{n}_a is given by the Bose distribution

$$\bar{n}_a = \frac{1}{e^{\hbar\omega/k_B T} - 1}$$

Since we are working in the optical frequencies (e.g. 10^{15} Hz), we can approximate the above expression as

$$\bar{n}_a \approx e^{-\hbar\omega/k_B T}$$

Obviously, for very high frequencies¹⁴ $\bar{n}_a \approx 0$ and thus our calculations in the previous section are still valid. However, now we also have to consider the correlation of

¹⁴For this reason, the laser is sometimes referred to as a reservoir with zero temperature.

$\langle \hat{a}_{in}^\dagger(\omega) \hat{a}_{in}(\omega') \rangle$. Here, we can no longer neglect the vacuum contribution

$$\begin{aligned}
\langle \hat{a}_{in}^\dagger(\omega) \hat{a}_{in}(\omega') \rangle &= 2\gamma_m \langle \hat{a}_{in}(t) \hat{a}_{in}^\dagger(t') \rangle + 2(\Gamma_m - \gamma_m) \langle \hat{a}_{in}(t) \hat{a}_{in}^\dagger(t') \rangle \\
2\gamma_m(n_a + 1)\delta(t - t') &= 2\gamma_m(\tilde{n}_a + 1)\delta(t - t') + 2(\Gamma_m - \gamma_m)(\bar{n}_a + 1)\delta(t - t') \\
&\approx 2\gamma_m(\tilde{n}_a + 1)\delta(t - t') + 2(\Gamma_m - \gamma_m)\delta(t - t') \\
&= 2\gamma_m \left(\tilde{n}_a + \frac{\Gamma_m}{\gamma_m} \right) \delta(t - t')
\end{aligned} \tag{47}$$

Thus, the only change that we have to make is to replace $n_a + 1$ in eq. (44) with $n_a + \Gamma_m/\gamma_m$.

Before we proceed with our calculations, there is one more detail to be considered. In section 2, we listed some of the fundamental assumptions of the Heisenberg-Langevin approach to quantum damping theory. Among those, was the assumption that the reservoir spectrum is flat. But the Planck distribution, which we used in our argument above, is certainly not flat. However, we know that the mechanical frequency of the membrane is significantly lower than the laser frequency ($\omega_m \ll \omega_L$). Thus, for a given temperature T the spectrum in the vicinity of the driving laser frequency (e.g. $\omega_L \pm \omega_m$) is practically flat.

4.2 Break-down of the rotating-wave approximation

We are now ready to complete our analysis. The inverse Fourier transformation of the creation and annihilation operators are

$$\begin{aligned}
\hat{b}(t) &= \sqrt{\frac{2\gamma_m}{2\pi}} \int_{-\infty}^{\infty} \frac{m_{3,1}(\omega) \hat{a}_{in}(\omega)}{\mathcal{D}(\omega)} e^{-i\omega t} d\omega + \sqrt{\frac{2\gamma_m}{2\pi}} \int_{-\infty}^{\infty} \frac{m_{3,2}(\omega) \hat{a}_{in}^\dagger(\omega)}{\mathcal{D}(\omega)} e^{-i\omega t} d\omega \\
&+ \sqrt{\frac{2\gamma}{2\pi}} \int_{-\infty}^{\infty} \frac{m_{3,3}(\omega) \hat{b}_{in}(\omega)}{\mathcal{D}(\omega)} e^{-i\omega t} d\omega + \sqrt{\frac{2\gamma}{2\pi}} \int_{-\infty}^{\infty} \frac{m_{3,4}(\omega) \hat{b}_{in}^\dagger(\omega)}{\mathcal{D}(\omega)} e^{-i\omega t} d\omega \\
\hat{b}^\dagger(t) &= \sqrt{\frac{2\gamma_m}{2\pi}} \int_{-\infty}^{\infty} \frac{m_{4,1}(\omega') \hat{a}_{in}(\omega')}{\mathcal{D}(\omega')} e^{-i\omega' t} d\omega' + \sqrt{\frac{2\gamma_m}{2\pi}} \int_{-\infty}^{\infty} \frac{m_{4,2}(\omega') \hat{a}_{in}^\dagger(\omega')}{\mathcal{D}(\omega')} e^{-i\omega' t} d\omega' \\
&+ \sqrt{\frac{2\gamma}{2\pi}} \int_{-\infty}^{\infty} \frac{m_{4,3}(\omega') \hat{b}_{in}(\omega')}{\mathcal{D}(\omega')} e^{-i\omega' t} d\omega' + \sqrt{\frac{2\gamma}{2\pi}} \int_{-\infty}^{\infty} \frac{m_{4,4}(\omega') \hat{b}_{in}^\dagger(\omega')}{\mathcal{D}(\omega')} e^{-i\omega' t} d\omega'
\end{aligned}$$

The mean occupation number for the LC-circuit is therefore

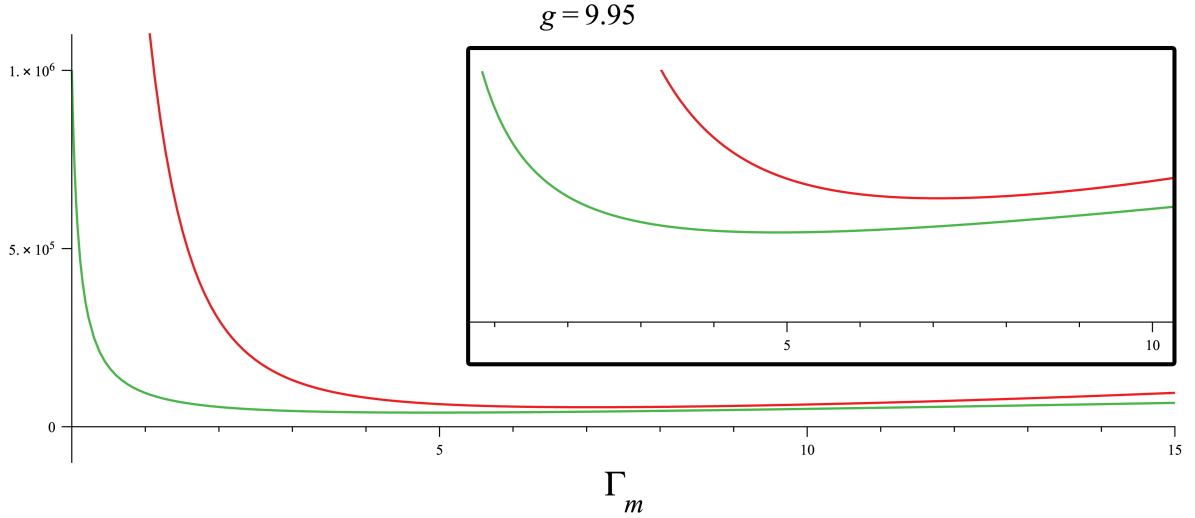
$$\begin{aligned}
\langle \hat{b}^\dagger \hat{b} \rangle &= \frac{2\gamma_m}{2\pi} \int_{-\infty}^{\infty} \int_{-\infty}^{\infty} \frac{m_{3,1}(\omega) m_{4,2}(\omega')}{\mathcal{D}(\omega) \mathcal{D}(\omega')} \langle \hat{a}_{in}^\dagger(\omega') \hat{a}_{in}(\omega) \rangle e^{-i(\omega+\omega')t} d\omega d\omega' \\
&+ \frac{2\gamma_m}{2\pi} \int_{-\infty}^{\infty} \int_{-\infty}^{\infty} \frac{m_{3,2}(\omega) m_{4,1}(\omega')}{\mathcal{D}(\omega) \mathcal{D}(\omega')} \langle \hat{a}_{in}(\omega') \hat{a}_{in}^\dagger(\omega) \rangle e^{-i(\omega+\omega')t} d\omega d\omega' \\
&+ \frac{2\gamma}{2\pi} \int_{-\infty}^{\infty} \int_{-\infty}^{\infty} \frac{m_{3,3}(\omega) m_{4,4}(\omega')}{\mathcal{D}(\omega) \mathcal{D}(\omega')} \langle \hat{b}_{in}^\dagger(\omega') \hat{b}_{in}(\omega) \rangle e^{-i(\omega+\omega')t} d\omega d\omega' \\
&+ \frac{2\gamma}{2\pi} \int_{-\infty}^{\infty} \int_{-\infty}^{\infty} \frac{m_{3,4}(\omega) m_{4,3}(\omega')}{\mathcal{D}(\omega) \mathcal{D}(\omega')} \langle \hat{b}_{in}(\omega') \hat{b}_{in}^\dagger(\omega) \rangle e^{-i(\omega+\omega')t} d\omega d\omega'
\end{aligned}$$

$$\begin{aligned}
&= \frac{2\gamma_m}{2\pi} \int_{-\infty}^{\infty} \frac{m_{3,1}(\omega)m_{4,2}(-\omega)}{\mathcal{D}(\omega)\mathcal{D}(-\omega)} n_a d\omega + \frac{2\gamma_m}{2\pi} \int_{-\infty}^{\infty} \frac{m_{3,2}(\omega)m_{4,1}(-\omega)}{\mathcal{D}(\omega)\mathcal{D}(-\omega)} \left(n_a + \frac{\Gamma_m}{\gamma_m}\right) d\omega \\
&+ \frac{2\gamma}{2\pi} \int_{-\infty}^{\infty} \frac{m_{3,3}(\omega)m_{4,4}(-\omega)}{\mathcal{D}(\omega)\mathcal{D}(-\omega)} n_b d\omega + \frac{2\gamma}{2\pi} \int_{-\infty}^{\infty} \frac{m_{3,4}(\omega)m_{4,3}(-\omega)}{\mathcal{D}(\omega)\mathcal{D}(-\omega)} (n_b + 1) d\omega \quad (48)
\end{aligned}$$

The integrals are evaluated exactly in the same manner as in section 3.3. We find the following 4 poles for $\mathcal{D}(\omega)$ (all the combinations of +/-)

$$\omega = -i\frac{\Gamma_m + \gamma}{2} \pm \frac{1}{2}\sqrt{4\tilde{\omega}^2 - (\Gamma_m - \gamma)^2 \pm 4\tilde{\omega}\sqrt{g^2 - (\Gamma_m - \gamma)^2}} \quad (49)$$

The remaining part of our analysis will be numeric, since the analytical expression for the occupation number is huge. Due to the fact that the vacuum contribution is taken into account in our calculations, some of the terms in the expression for the occupation number are "independent" of the reservoir excitation numbers n_a and n_b . Thus we consider the population number for specific values of n_a and n_b - in our case, $n_a = n_b = 10^6$. Furthermore, $\tilde{\omega} = 10 \text{ s}^{-1}$. In the following illustrations the solution without the rotating-wave approximation is being compared to the exact solution from section 3.3 (see eq. (37)). The latter is indicated with a green color



The first plot clearly shows a difference between the solution with and without the rotating-wave approximation. In the corner we have zoomed in at the minimum point and as we can see, the optimal damping rate is slightly higher than predicted by the exact solution with the RWA.

The second illustration is quite interesting (see Figure 9), since it indicates that for $g/\tilde{\omega} \approx 0.7$ (and below) the exact solution from section 3.3 is a reasonable approximation in the vicinity of the minimum. In fact, for $g/\tilde{\omega} \approx 0.7$ the minimum occupation numbers for the solution without RWA is approximately 10% higher (i.e. the relative percentage difference) than the occupation number according to eq. (37).

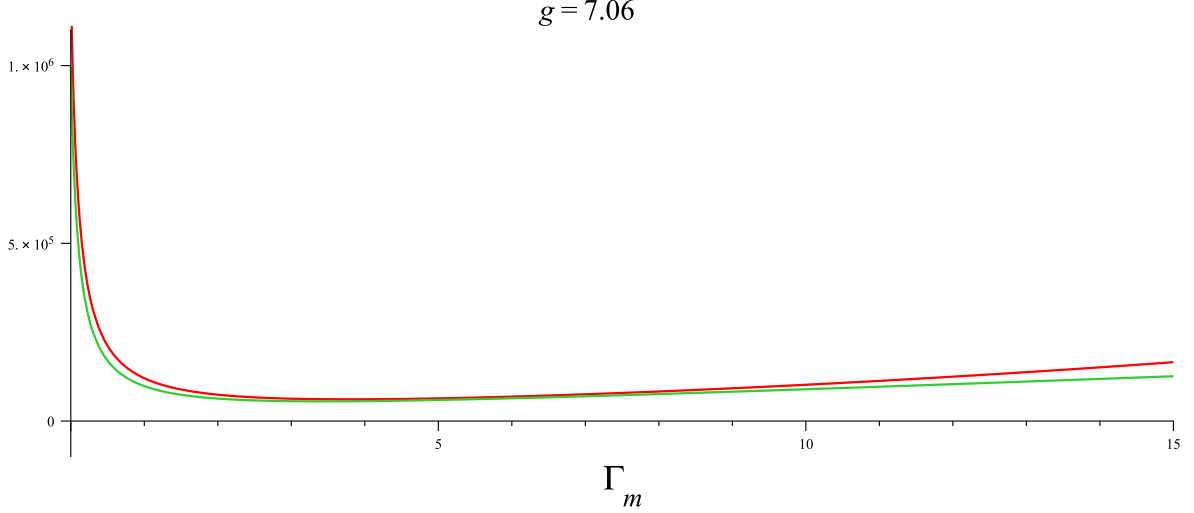


Figure 9: Occupation number of the LC-circuit. Here $\omega = 10 \text{ s}^{-1}$, $\gamma_m = 10^{-4} \text{ s}^{-1}$, $\gamma = 0.1 \text{ s}^{-1}$ and $n_a = n_b = 10^6$.

Finally, we consider the limit $g \approx \tilde{\omega}$

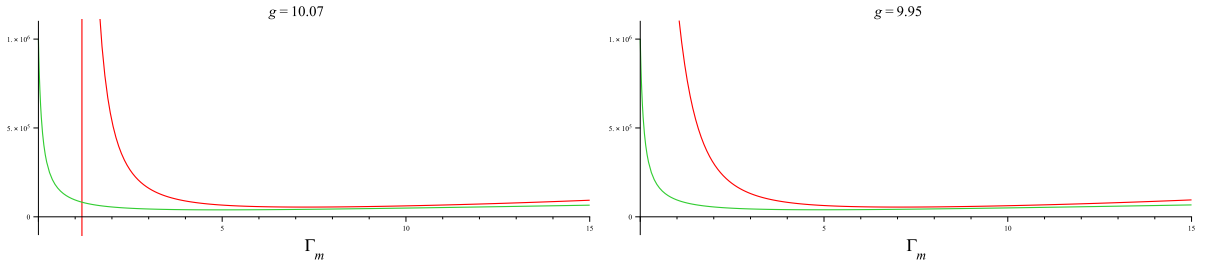


Figure 10: Occupation number of the LC-circuit. Here $\omega = 10 \text{ s}^{-1}$, $\gamma_m = 10^{-4} \text{ s}^{-1}$, $\gamma = 0.1 \text{ s}^{-1}$ and $n_a = n_b = 10^6$.

As we can see the exact solution without the rotating-wave approximation breaks down for $g > \tilde{\omega}$ (e.g. the solution suggests negative occupation number). A simple consideration can in fact help us understand the reason why our solution is no longer valid for $g > \tilde{\omega}$. We recall that the time-evolution in the Schrödinger picture is a simple exponential function[9, p.26]

$$e^{-iEt/\hbar} = e^{-i\omega t}$$

If we insert one of the poles from eq. (48) in the expression above, we get an exponential decay term $\exp(-(\Gamma_m + \gamma)/2)$ and an oscillating term. However, for certain values of the coupling constant g the poles can become positive complex numbers. This corresponds to solving $\omega = 0$ for $\tilde{\omega}$

$$i \frac{\Gamma_m + \gamma}{2} = \frac{1}{2} \sqrt{4\tilde{\omega}^2 - (\Gamma_m - \gamma)^2 - 4\tilde{\omega} \sqrt{g^2 - (\Gamma_m - \gamma)^2}}$$

$$\tilde{\omega} = \frac{1}{2} \left(\sqrt{g^2 - (\Gamma_m - \gamma)^2} + \sqrt{g^2 - (\Gamma_m \gamma)^2} \right)$$

we set $\Gamma_m = 0$ and arrive at the following result

$$\tilde{\omega} = \sqrt{g^2 - \gamma^2} \approx g$$

This means that for $g > \tilde{\omega}$ we have *negative* decay rates, which of course is unphysical. Thus our solution is only valid for $g < \tilde{\omega}$.

5 Discussion and outlook

Although we have analysed the coupling between the membrane and the LC-circuit both in the limiting cases as well as with and without the rotating-wave approximation, there are still a number of possibilities for further analysis. First and foremost, an analytical expression for the occupation number is desirable (for the calculation without RWA).

One of the most natural ways to extend our analysis would be taking the coupling between the cavity and membrane into account. Mathematically this could be done by adding the following two terms to our Hamiltonian in eq. (22)

$$\hat{H}_{cav} = \omega_{cav} \hat{c}^\dagger \hat{c} + \frac{f}{2} (\hat{a} + \hat{a}^\dagger) (\hat{c} + \hat{c}^\dagger) \quad (50)$$

Similar to the approach in this thesis, the analysis of the cavity/membrane/LC-system could be extended by omitting the rotating-wave approximation.

As we can see, the analysis can be extended in various ways. Each providing a more detailed picture of our system.

6 Conclusion

The objective of this bachelor's thesis has been to carry out a full derivation of the LC occupation number using the Heisenberg-Langevin formalism. In the rotating-wave approximation we showed that for $g \gg \gamma_m, \gamma$ the optimal external damping rate Γ_m is $g/2$, in accordance with the results presented in [1]. Furthermore, the minimum relative occupation number was found to be $4\gamma/g$. This result differs from the approximate expression for the minimum occupation number by a factor of 2.

We analyzed the coupling between the mechanical oscillator and the LC-circuit without the rotating-wave approximation. Despite the fact that we were unable to find a compact analytical expression, we found that the derivation is only valid for $g < \omega$ (otherwise negative decay rates are introduced). Furthermore, we found that for approximately $g/\omega \leq 0.7$ the occupation number derived using the rotating-wave approximation provides a reasonable description of the number of excitations in the LC-circuit.

References

- [1] J.M. Taylor, A.S. Sørensen, C.M. Marcus, E.S. Polzik: *Laser Cooling and Optical Detection of Excitations in a LC Electrical Circuit*, Phys. Rev. Lett. 107, (2011)
- [2] V.B. Braginsky, A.B. Manukin: *Ponderomotive effects of electromagnetic radiation*, Sov. Phys. JETP, 25:653 (1967)
- [3] Peter. W. Milonni, Joseph H. Eberly: *Laser Physics* (2010)
- [4] C.W. Gardiner, P. Zoller: *Quantum Noise*, Second Enlarged Edition (2000)
- [5] C.W. Gardiner, M.J. Collett: *Input and output in damped quantum systems: Quantum stochastic differential equations and the master equation*, Phys. Rev. A 31, (1985)
- [6] J.D. Thompson, B.M. Zwickl, A.M. Jayich, Florian Marquardt, S.M. Girvin, J.G.E. Harris: *Strong dispersive coupling of a high-finesse cavity to a micromechanical membrane*, Nature 452, (2008)
- [7] K.F. Riley, M.P. Hobson, S.J. Bence: *Mathematical Methods For Physics And Engineering*, Third Edition (2006)
- [8] H. Haken: *Synergetics: Introduction and Advanced Topics*, 3rd Revised Edition (2004)
- [9] D.J. Griffiths: *Introduction to Quantum Mechanics*, Second Edition (2005)

A Solutions with RWA

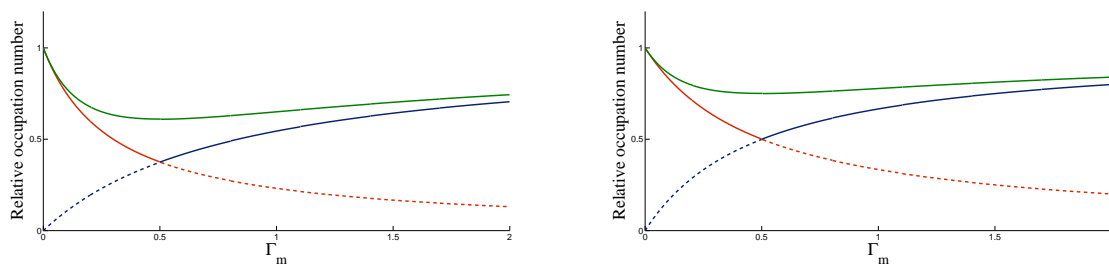


Figure 11: Left: $\gamma_m = 10^{-4} \text{ s}^{-1}$, $\gamma = 0.3 \text{ s}^{-1}$ and $g = 1 \text{ s}^{-1}$. Right: $\gamma_m = 10^{-4} \text{ s}^{-1}$, $\gamma = 0.5 \text{ s}^{-1}$ and $g = 1 \text{ s}^{-1}$.

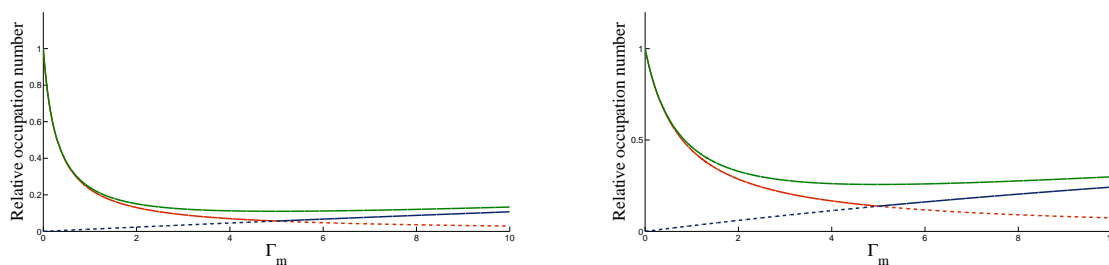


Figure 12: Left: $\gamma_m = 10^{-4} \text{ s}^{-1}$, $\gamma = 0.3 \text{ s}^{-1}$ and $g = 10 \text{ s}^{-1}$. Right: $\gamma_m = 10^{-4} \text{ s}^{-1}$, $\gamma = 0.8 \text{ s}^{-1}$ and $g = 10 \text{ s}^{-1}$.

B Entries of the inverted 4x4 matrix

Here the entries of \mathbf{M}^{-1} are listed

$$\begin{aligned}
m_{1,1} &= (\Gamma_m - i\tilde{\omega} - i\omega) (\gamma + i\tilde{\omega} - i\omega) (\gamma - i\tilde{\omega} - i\omega) + i\frac{g^2}{2}\tilde{\omega} \\
m_{1,2} &= i\frac{g^2}{2}\tilde{\omega} \\
m_{1,3} &= i\frac{g}{2}(\Gamma_m - i\tilde{\omega} - i\omega) (\gamma - i\tilde{\omega} - i\omega) \\
m_{1,4} &= i\frac{g}{2}(\Gamma_m - i\tilde{\omega} - i\omega) (\gamma + i\tilde{\omega} - i\omega) \\
m_{2,1} &= -i\frac{g^2}{2}\tilde{\omega} \\
m_{2,2} &= (\Gamma_m + i\tilde{\omega} - i\omega) (\gamma + i\tilde{\omega} - i\omega) (\gamma - i\tilde{\omega} - i\omega) - i\frac{g^2}{2}\tilde{\omega} \\
m_{2,3} &= -i\frac{g}{2}(\Gamma_m + i\tilde{\omega} - i\omega) (\gamma - i\tilde{\omega} - i\omega) \\
m_{2,4} &= -i\frac{g}{2}(\Gamma_m + i\tilde{\omega} - i\omega) (\gamma + i\tilde{\omega} - i\omega) \\
m_{3,1} &= i\frac{g}{2}(\Gamma_m - i\tilde{\omega} - i\omega) (\gamma - i\tilde{\omega} - i\omega) \\
m_{3,2} &= i\frac{g}{2}(\Gamma_m + i\tilde{\omega} - i\omega) (\gamma - i\tilde{\omega} - i\omega) \\
m_{3,3} &= (\Gamma_m + i\tilde{\omega} - i\omega) (\Gamma_m - i\tilde{\omega} - i\omega) (\gamma - i\tilde{\omega} - i\omega) + i\frac{g^2}{2}\tilde{\omega} \\
m_{3,4} &= i\frac{g^2}{2}\tilde{\omega} \\
m_{4,1} &= -i\frac{g}{2}(\Gamma_m - i\tilde{\omega} - i\omega) (\gamma + i\tilde{\omega} - i\omega) \\
m_{4,2} &= -i\frac{g}{2}(\Gamma_m + i\tilde{\omega} - i\omega) (\gamma + i\tilde{\omega} - i\omega) \\
m_{4,3} &= -i\frac{g^2}{2}\tilde{\omega} \\
m_{4,4} &= (\Gamma_m + i\tilde{\omega} - i\omega) (\Gamma_m - i\tilde{\omega} - i\omega) (\gamma + i\tilde{\omega} - i\omega) - i\frac{g^2}{2}\tilde{\omega}
\end{aligned}$$

C Solutions without RWA

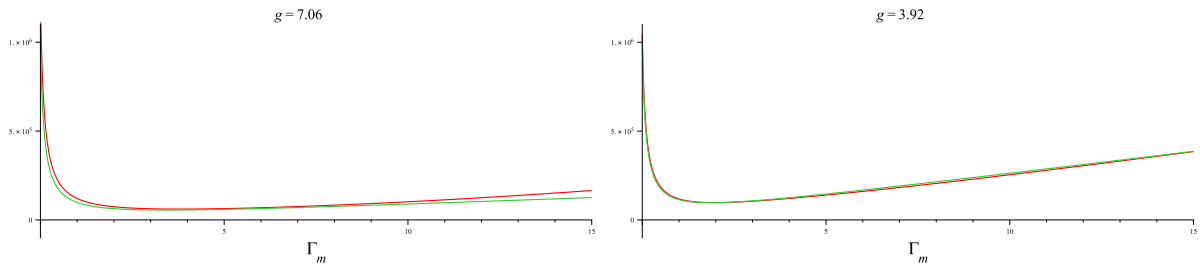


Figure 13: $\gamma_m = 10^{-4} \text{ s}^{-1}$, $\gamma = 0.1 \text{ s}^{-1}$ and $\tilde{\omega} = 10 \text{ s}^{-1}$.

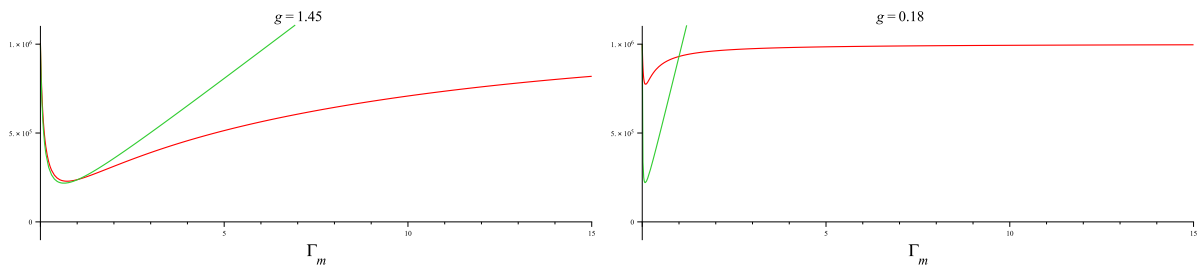


Figure 14: $\gamma_m = 10^{-4} \text{ s}^{-1}$, $\gamma = 0.1 \text{ s}^{-1}$ and $\tilde{\omega} = 10 \text{ s}^{-1}$.